Development of a Machine Learning Model for Aspyre Lung Blood: A New Assay for Rapid Detection of Actionable Variants From Plasma in Patients With Non–Small Cell Lung Cancer

Rebecca N. Palmer, PhD[1]; Sam Abujudeh, BEng, MPhil, PhD[1]; Magdalena Stolarek-Januszkiewicz, PhD[1]; Ana-Luisa Silva, PhD[1]; Justyna M. Mordaka, PhD[1]; Kristine von Bargen, PhD[1]; Alejandra Collazos, PhD[1]; Simonetta Andreazza, PhD[1]; Nicola D. Potts, PhD[1]; Chau Ha Ho, PhD[1]; Iyelola Turner, BSc, MSc, PhD[1]; Jinsy Jose, MSc[1]; Dilyara Nugent, MSc[1]; Prarthna Barot, BSc, MSc[1]; Christina Xyrafaki, PhD[2]; Alessandro Tomassini, PhD[1]; Ryan T. Evans, MSc, PhD[2]; Katherine E. Knudsen, PhD[2]; Elizabeth Gillon-Zhang, BSc[2]; Julia N. Brown, BSc[2]; Candace King, BSc[2]; Cory Kiser, BS[2]; Mary Beth Rossi, BS[2]; Eleanor R. Gray, MSc, MBiochem, PhD[1]; Robert J. Osborne, BSc, PhD[1]; and Barnaby W. Balmforth, MPhys, PhD[1]

DOI https://doi.org/10.1200/CCI-25-00050

ABSTRACT

PURPOSE Aspyre Lung is a targeted biomarker panel of 114 genomic variants across 11 guideline-recommended genes with simultaneous DNA and RNA for non–small cell lung cancer (NSCLC). In this study, we developed a machine learning algorithm to interpret fluorescence data outputs from Aspyre Lung, enabling the assay to be applied to both plasma and tissue samples.

MATERIALS AND METHODS Data for model training and testing were generated from over 13,500 DNA and RNA contrived samples, with variants spiked in at a variant allele frequency (VAF) of 0.1%-82% for DNA and 6-5,000 copies for RNA. The training and testing data sets used 67 reagent batches and 23 operators using nine quantitative polymerase chain reaction machines at two sites. Variant calling machine learning models were assessed in terms of median assay-wide 95% limit of detection (LoD95), observed sensitivity, false-positive rate per sample, per-variant LoD95, and per-variant observed sensitivity. The model was optimized by varying the training data subsets, features used, and model hyperparameters. Models were assessed against target specifications.

RESULTS Verification with reference samples established experimental performance characteristics: a LoD95 of 0.19% VAF for SNV/indels, one amplifiable copy for gene fusions, 69 copies for *MET* exon 14 skipping events, and 100% specificity for all targets.

CONCLUSION Implementation of the model for liquid biopsy sample analysis enables running of these samples alongside tissue in a single workflow with high sensitivity, specificity, and accuracy. These results demonstrate that the Aspyre Lung assay, powered by a robust machine learning algorithm, offers a reliable and scalable solution for molecular testing in NSCLC, enabling a diverse range of laboratories to confidently perform high-sensitivity, high-specificity testing on both tissue and liquid biopsy samples.

ACCOMPANYING CONTENT

- Data Sharing Statement
- Data Supplement

Accepted July 11, 2025
Published August 15, 2025

JCO Clin Cancer Inform
9:e2500050

INTRODUCTION

Guidelines recommend biomarker testing for target genes in non–small cell lung cancer (NSCLC).[1] Targeted therapies linked to actionable mutations can significantly improve patient outcomes[1]; however, results must be promptly received and appropriately interpreted as starting nontargeted standard cytotoxic chemotherapy compromises outcomes even if followed by targeted therapy.[2,3]

Liquid biopsy analysis of circulating cell-free DNA (cfDNA) and RNA (cfRNA) from blood is minimally invasive and potentially transformative for molecular profiling. Liquid biopsy can be performed in cases where tissue is unavailable or insufficient for molecular analysis, often with faster turnaround times, and is recommended as an alternative or complementary approach for patients with insufficient or unavailable tissue or when turnaround time is critical.[1,4] Adoption is limited, however, by availability of plasma-

CONTEXT

Key Objectives

To develop and test an algorithm for interpretation of real-time fluorescence data from isothermal rolling circle amplification of circularized probes after pyrophosphorolytic degradation, generated from running the Aspyre Lung assay on cell-free DNA (cfDNA) and cell-free RNA (cfRNA) from blood.

Knowledge Generated

Our study developed and validated a support vector machine learning algorithm to yield variant calls for all 114 biomarkers analyzed with 95% limit of detection 0.19% for cfDNA variants and six copies of gene fusions from cfRNA. Optimization involved exploring the impact of changing the training data set, the included probe interactions, and model parameters.

Relevance *(Z. Bakouny)*

Molecular testing has become an essential part of management for non-small-cell lung cancer, yet the available tests are not always available in resource-poor settings, and even when tests are available, they sometimes have long turnaround times. In this study, the authors develop a computational machine-learning-based algorithm to analyze data from a liquid biopsy test that is less resource intensive and can have faster turnaround time. Such tests promise to further democratize the advances of precision oncology.*

*Relevance section written by *JCO CCI* Associate Editor Ziad Bakouny, MD, MSc.

based assays that meet stringent analytical and clinical requirements.

Next-generation sequencing (NGS) technologies applied to tissue and liquid biopsies have revolutionized biomarker testing in oncology. NGS-based assays can detect a wide range of genetic variants, making them well-suited for discovery-based applications and comprehensive molecular profiling. Currently, two NGS-based liquid biopsy assays for patients with NSCLC are Food and Drug Administration–approved (and others for solid tumors); however, gaps persist in molecular profiling.[5] NGS utility in clinical settings is often constrained by its resource-intensive nature, requiring specialized equipment, highly skilled personnel, and advanced bioinformatics infrastructure. Consequently, NGS testing is predominantly performed in reference laboratories and larger tertiary care centers, limiting availability, raising costs, and lengthening turnaround times for patients.[6] Even when coverage exists, testing rates can be well under 50%, with high failure rates.[6-9] Around 26% of patients remain untested before treatment initiation[3]; among the 50% who receive biomarker results, 27%-29% do not receive appropriate targeted treatment,[5,10] suggesting that 64% of eligible patients with NSCLC are excluded from tailored therapies.[5,11] Simpler testing techniques are limited by poor sensitivity and multiplexing (real-time polymerase chain reaction [PCR]) or restricted multiplexing (digital PCR [dPCR]).

To address these challenges, we developed Aspyre Lung (Tissue) and (Blood) assays, covering all first-line targets in NSCLC. The technology uses pyrophosphorolysis (reverse DNA polymerization), which is exquisitely specific for perfectly double-stranded DNA, enabling discrimination between wild-type and variant-containing sequences using rationally designed probes in a parallelized workflow for DNA and RNA. Detection of single nucleotide variants (SNVs) and indels from DNA is possible alongside RNA-based detection of gene fusions and exon skipping.[12-14] The reagents and protocol are identical for tissue and blood, sampling DNA and RNA[12] or cfDNA and cfRNA.[14] Assay equipment comprises a thermocycler and real-time PCR, lowering the bar for decentralization into local laboratories.

Unlike quantitative PCR (qPCR) fluorescence data analysis using well-established methods,[15,16] the real-time data generated from isothermal amplification of circularized probes after pyrophosphorolytic degradation are unique to Aspyre, with consequently no standards. Complexities include probe interactions, competition for reagents, optical overlap of emission spectra, x-y locational plate effects, reagent batch effects, and curve fitting and interpretation. Some challenges mirror those of other fluorescence methodologies, whereas others are unique to Aspyre. Methods developed herein could be applied to other amplification methodologies, potentially improving performance metrics.

Previously, we reported single-color assays with one variant per well[17] and four-color assays with simple baseline correction and then fitting based on previous methods.[13] Support vector machine (SVM) learning algorithms were implemented to analyze and classify data from formalin-fixed paraffin-embedded (FFPE) tissue, calling variants with high accuracy.[12] This study extends the SVM to plasma

samples, refining machine learning models to meet stringent sensitivity and specificity requirements for liquid biopsy. We describe optimization and validation of models to facilitate rapid, accurate, minimally invasive genomic profiling.

MATERIALS AND METHODS

Reference Samples

Variant-positive samples (Data Supplement) were prepared by spiking variant-containing oligonucleotides into variant-free DNA or RNA background and quantified.[12] cfDNA derived from healthy donor blood, DNA from FFPE tonsil tissue, and genomic DNA (gDNA) were used as backgrounds for contrived samples, quantified using Qubit and dPCR. cfRNA derived from healthy donor blood and RNA from FFPE tonsil tissue were used as RNA backgrounds and quantified using Qubit. To achieve required variant allele frequency (VAF) or copies, samples were serially diluted and stored at −20°C (DNA) or −80°C (RNA).

Nucleic Acid Extraction

cfDNA/cfRNA were extracted from plasma samples, and DNA and RNA were extracted from FFPE tonsil blocks as described previously.[12,14] Nucleic acid concentrations were measured as described previously.[12,14]

Aspyre Lung Reactions

Aspyre Lung assays were run as in the studies by Evans et al[12,14] by 23 operators using 67 reagent batches for training and model evaluations. Standard/low input levels were 20 ng/5 ng of cfDNA and 42 ng/6 ng of cfRNA, respectively. Data were downloaded from QuantStudio 5 Real-Time 384 PCR Systems (Thermo Fisher, Waltham, MA) and exported using DA2 software v.2.6 or 2.7 (Thermo Fisher). Raw data comma separated values were used during training, thresholding, or testing machine learning models.

Limit of Blank (Standard and Low Input)

Samples from 50 independent healthy donors were used: cfDNA and cfRNA were not always matched because of availability. A total of 120 samples from 30 independent healthy volunteers were each run four times at low input; 56 samples from 22 (cfDNA) and 27 (cfRNA) independent healthy volunteers were tested at standard input. Eleven runs were executed by four operators using two batches of reagents and five different QuantStudio five machines. Reduced input and standard samples were treated identically, and real-time runs comprised a mix of both.

Limit of Detection

Fourteen DNA and 14 RNA variants were selected (Data Supplement). Four levels of VAF or copy number and 15 repeats of each were tested using six reagent batches and analyzed using the final models. Three double-mutant DNA samples were tested with six replicates per reagent batch (Data Supplement). Per-variant 95% limit of detection (LoD95) was established as the lowest test level with ≥95% hit rate or estimated from linear regression analysis. Thirty-one DNA and 24 RNA wild-type samples per batch were also tested. Nine operators performed experiments using six QuantStudio5 Real-Time PCR machines.

Data Analysis

Aspyre Lung experimental output comprises 96 real-time fluorescence curves per sample collected over 200 measurements. One curve mostly corresponds to one variant, but correspondence is imperfect. Curves are sigmoidal, or flat, and inflexion point(s) occurs earlier when the target is present and later or absent if not present (Data Supplement). A description of data preprocessing and variant calling steps is illustrated in Figure 1 and expanded in the Data Supplement. Output results for each reportable variant are "detected," "not detected" or "undetermined." An output may be one sequence-level variant, or a group of sequence-level variants that are not distinguished (eg, *ERBB2* p.Y772_A775dup for COSM20959/COSM12558). Each DNA sequence-level variant has an independent probe and curve. Reportable variants for RNA are driver genes (3′ portion of the gene fusion), with one curve potentially fed by multiple probes.

RESULTS

Setting of Target Specifications

Dilution of tumor-derived nucleic acids by wild-type results in lower variant DNA and RNA levels in plasma compared with tissue.[6,18,19] Aspyre is capable of performing single molecule detection,[13,17] and hence, modifications for liquid biopsy adaptation were made to data analysis, balancing sensitivity with specificity. Target specifications for Aspyre Lung Blood were set using the published literature and competitor analysis[18] (Table 1).

Generation of Data for Training and Testing

Production of a large training data set using background cfDNA and cfRNA from healthy volunteers would be prohibitive. We instead performed comparator studies showing that gDNA from lymphoblastoid cell lines and RNA from FFPE tonsil tissue are suitable proxies for cfDNA and cfRNA, respectively (Data Supplement). A large-scale set of experiments generated data to design, train, and test an SVM for variant calling with 6,908 DNA and 6,606 RNA samples across 67 reagent batches and nine qPCR machines. The target DNA VAFs across experiments were 0.1%-82%, and 6-5,000 copies of variants that are detected from RNA.

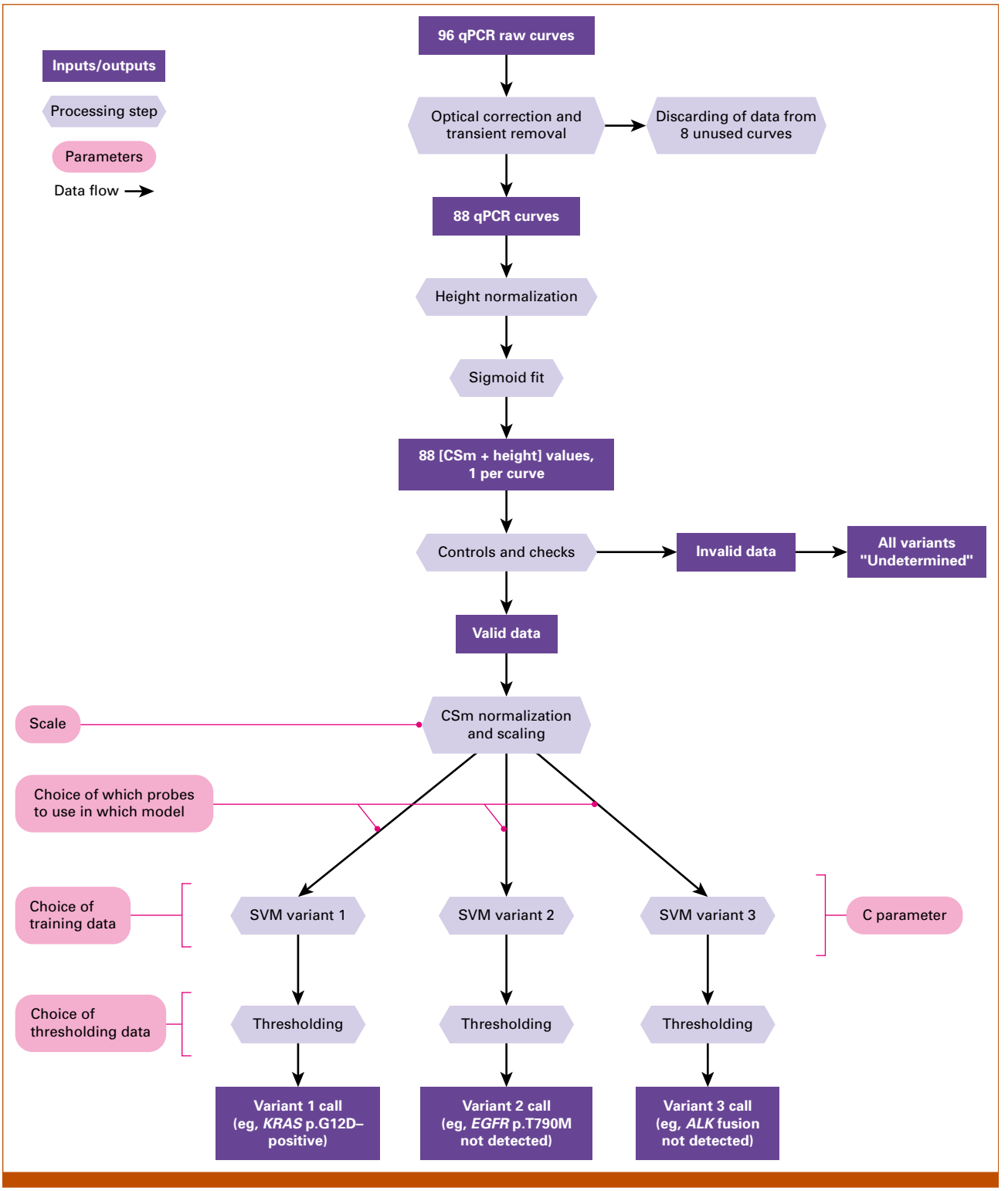

FIG 1. Schematic of the data processing stages of Aspyre Lab, taking input of real-time fluorescence data from qPCR thermocyclers and producing output of calls for each variant in the Aspyre Lung assay. Each SVM model uses a subset of probes, and these subsets may be of different sizes. For clarity, only three probes and three variants are shown; there are actually 71 reportable variants using a total of 86 probes. All parameters were chosen inputs set for each SVM model run; the outputs from each run are then assessed against the target specifications for the model (eg, sensitivity and specificity). CSm, Cycle of Sigmoid Midpoint; qPCR, quantitative polymerase chain reaction; SVM, support vector machine.

TABLE 1. Target Specifications for Aspyre Lung Blood Assay

Nucleic Acid	Class	Criteria	Desirable	Acceptable
DNA	SNVs and indels	Median panel-wide LoD95 (VAF)	0.45%	0.8%
RNA	Fusions	Median panel-wide LoD95 (amplifiable copies)	12	48
	MET exon 14 skipping	LoD95 (amplifiable copies)	120	200
DNA/RNA	Panel-wide	Per-sample FPR	0.3%	0.4%
		Median per-variant FPR	3×10^{-5}	3.45×10^{-5}

Abbreviations: FPR, false-positive rate; LoD95, 95% limit of detection; SNV, single nucleotide variant; VAF, variant allele frequency.

Development and Optimization of Variant Calling

In this study, we optimized the following SVM parameters: (1) training set (Data Supplement); (2) probes used for variant calling. Each variant detected at the nucleotide level has at least one directly associated oligonucleotide probe. The presence of a variant in a sample affects both its directly associated probe and potentially others, and therefore, performance benefits may result from using multiple probe signals to make variant calls; (3) C - regularization parameter, controlling trade-off between the hyperplane margin and misclassifications. Larger values of C favor a low error rate on training data, at a risk of overfitting and increasing error rate on other data, whereas smaller values of C favor a wider margin, potentially improving generalizability to unseen data; (4) scale - divides normalized parameters of Cycle of Sigmoid Midpoint (CSm) and S-curve height.

Combinations of parameter values were tested, and performance indicators are given in the Data Supplement (DNA and RNA). Numbers of tested models ran into the hundreds; tables are limited to models that performed better than tissue models.[12] Figure 2 shows key performance indicators, illustrating effects of varying probe sets for training DNA variant models. Probe Set 2 models (ie, features derived from their directly associated probe(s), probes with known cross-reactivity, and those that may physically interact in the assay) tended to have the highest sensitivity. While the probe set showed the most striking link to sensitivity, other parameters (C, scale, training set) also had an effect (Data Supplement). Models using all DNA probes (excluding driver and resistance combinations, Set 3) tended to have lower sensitivity for multivariant samples relative to single variant samples. In addition, models using Probe Set 3 tended to have lower false-positive rates for variant-positive samples and relatively higher false-positive rates for variant-free samples. Probe Sets 1 and 2 did not exhibit this characteristic.

Figure 3 illustrates effects of varying training data sets on models for variants detected from RNA. During generation, it became apparent that the probe manufacturer had supplied contaminated oligonucleotides, meaning that one variant had much faster wild-type CSm in the affected batch than other batches. The machine learning algorithms hence chose a faster threshold to avoid false positives, reducing sensitivity. After working with the supplier to remove cross-contamination, this strict threshold was no longer necessary. Removal of cross-contaminated data from the training set allowed the model to learn this, increasing sensitivity to yield a median LoD95 for gene fusions of one amplifiable molecule. While the training set used showed the most striking link to sensitivity, other parameters (C, scale, probe set) also had an effect (Data Supplement).

All models were assessed against target specifications (Table 1) and relative to each other (Data Supplement) by comparing associated metrics. All models were designed to have the same specificity (Determination of Model Thresholds, Data Supplement). Table 2 shows final chosen model metrics; the median LoD95 across all DNA variants was 0.44% ± 0.16% and similar within classes: 0.44% ± 0.08% and 0.44% ± 0.21% for SNVs and multinucleotide variations (MNVs)/indels, respectively.

Verification of the LoD95 of the Final Model

Selected DNA and RNA models were combined and tested on unseen data including 14 DNA variants at four VAFs (SNV, MNV, and indels), 14 RNA variants at four copy numbers (gene fusions and *MET* exon 14 skipping), and three samples with two DNA variants. The LoD95 per variant was established as the lowest tested level with at least a 95% hit rate (effectively 15/15 positive replicates) and estimated from linear regression for variants individually and across classes. The LoD95 estimated from hit rate varied between 0.1% and 0.4% VAF for SNVs, 0.1% and 1% VAF for indels, 6 and 36 copies for gene fusions, and 160 copies for *MET* exon 14 skipping. A median assay-wide LoD95 based on hit rate was established at 0.2% VAF for SNV/indels and six copies for RNA fusions. The estimated LoD95 from linear regression was 0.19% VAF for SNV/MNVs/indels, one amplifiable copy for RNA fusions, and 15 copies of *MET* exon 14 skipping events (Table 3). Across the study, there was a single false-positive gene fusion result from a wild-type sample, potentially because of cross-contamination from variant-positive samples for this gene fusion in the same run.

Aspyre Lung (Blood) Is Highly Specific at Low Input Levels

Aspyre Lung (Blood) was initially optimized for 20 ng of cfDNA and 42 ng of cfRNA. Yields of nucleic acids from

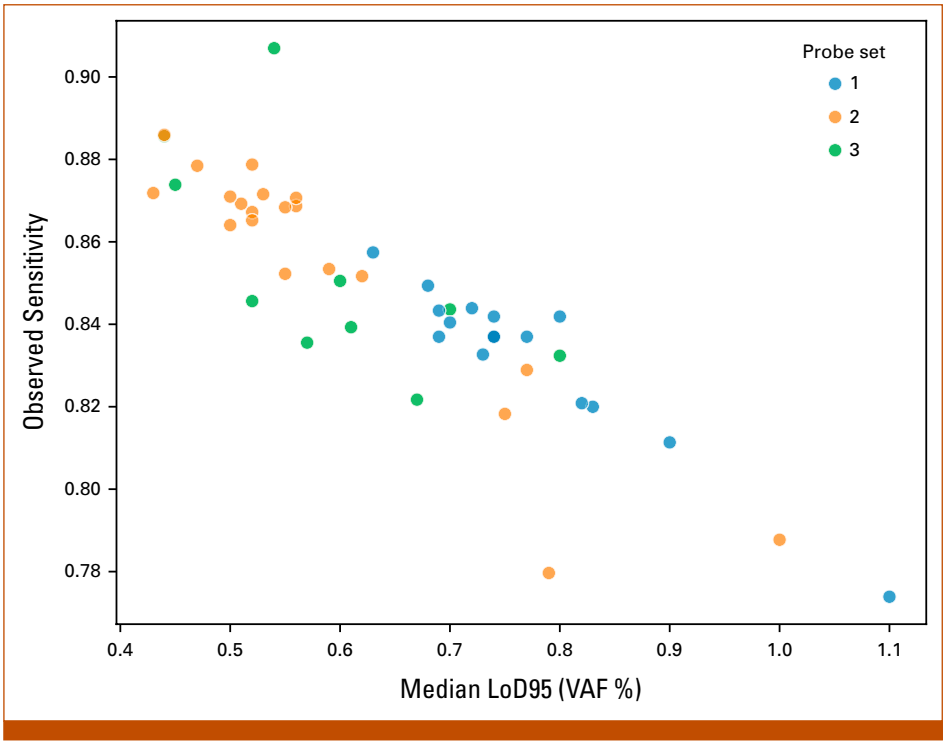

FIG 2. Effect of varying the probes used to call variants on estimated median LoD95 (across all DNA variants in the assay) and observed sensitivity. LoD95 is an estimated metric derived from outputs from the models, and observed sensitivity is computed across all variants from the test data; as expected, these are correlated but not perfectly, and placement toward the top left of the graph is generally better. Each point represents a unique combination of parameters (training set, probe set, C, scale) that were used to train each DNA variant calling model in the assay. Each point is colored by the probe set used: 1 (blue) includes only directly associated probe(s) and probes with known cross-reactivity for each variant; 2 (orange) includes directly associated probe(s), probes with known cross-reactivity, and those that physically interact in the assay; 3 (green) includes all DNA probes of the assay (excluding driver-drug resistance combinations) for each variant. Probe Set 2 generally performs best although other variables can have a large effect on performance (Data Supplement). LoD95, 95% limit of detection; VAF, variant allele frequency.

plasma depend on the patient, cancer stage, and tumor shedding profile,[20] with some yielding below recommended inputs. These can nonetheless provide clinically relevant variant calls if specificity is unaffected. Specificity was tested using cfDNA and cfRNA extracted from 50 variant-free blood samples. There were no positive calls of 20,064 variants analyzed in 176 samples at either input level (Table 4). The per-sample false-positive rate was 0% (0%-2.1% Clopper-Pearson 95% CI), supporting reduced input to 5 ng of cfDNA and 6 ng of cfRNA when standard inputs are unavailable.

DISCUSSION

Aspyre Lung (Blood) provides a noninvasive alternative to tissue biopsy, aligning with National Comprehensive Cancer Network and International Association for the Study of Lung Cancer recommendations.[1,4] Experimental assay outputs are sigmoidal fluorescence curves, similar to qPCR, although etiology, processing, and interpretation differ. Assay target specifications were intentionally clinically appropriate though technically challenging, requiring production of extensive training data and optimization of machine learning models. After model finalization, we produced independent verification data to ensure that performance met target specifications.

Probe sets strongly affected DNA model performance. In theory, including more probes allows each variant model to learn previously unknown probe cross-reactivity and subtle interactions for more accurate calls. Probe Set 3 models (used most or all DNA probes to call each DNA variant) had poorer relative performance for multivariant samples compared with single mutation samples and a relatively increased false-positive rate for variant-free versus variant-positive samples. This may be due to bias of training data toward samples with one mutation, and hence, the model learned to treat the apparent presence of another variant as evidence of the absence of its own variant. This reduces not only false-positive rates in variant-positive samples, as the potential false positive appears to be a second mutant, but also the sensitivity to real multivariant samples. This mechanism only operates when the model for the second mutant (or

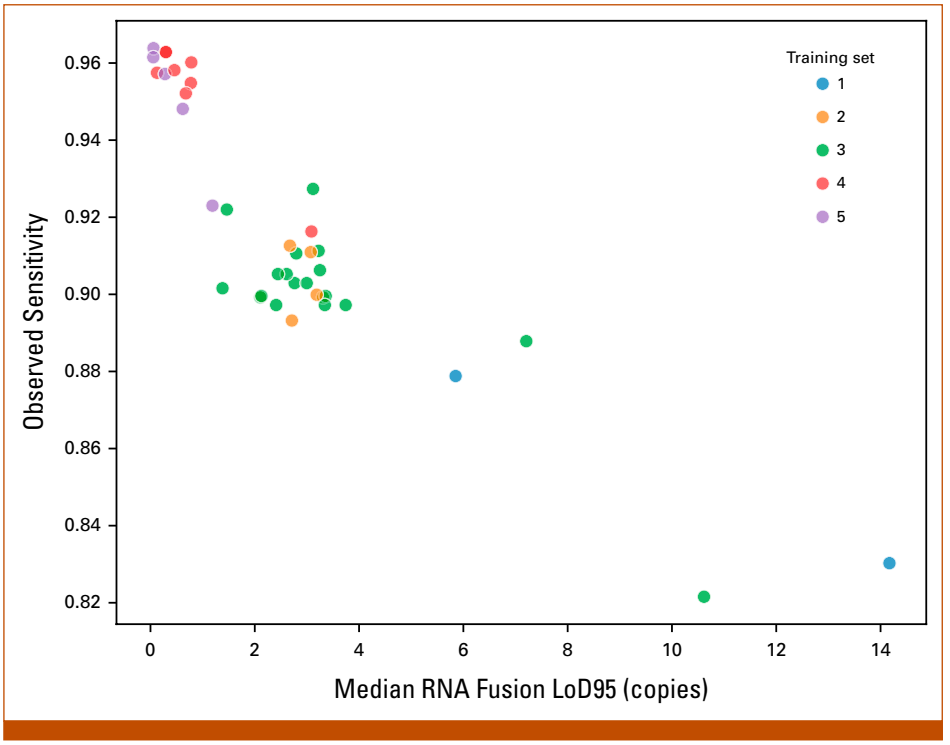

FIG 3. Effect of varying the training set used to call variants on estimated median RNA Fusion LoD95 (across all RNA fusion variants in the assay) and observed sensitivity. Each point represents a unique combination of parameters (training set, probe set, C, scale) that were used to train each RNA variant calling model in the assay. Each point is colored by the training set used: Set 1: Original FFPE training set; Set 2: Set 1 plus additional data set containing plasma-like samples; Set 3: Set 2 excluding FFPE DNA samples; Set 4: Set 3 excluding *some* data generated before lock of reagent manufacturing procedures; Set 5: Set 3 excluding *all* data before lock of reagent manufacturing procedures. FFPE, formalin-fixed paraffin-embedded; LoD95, 95% limit of detection.

potential false positive) includes one or more probes that significantly respond to the first mutant. This effect was not seen for Probe Set 1 and 2 models, likely because of them using fewer probes.

Consequently, composition of the thresholding set (variant-positive *v* variant-free samples) is crucial. When determining thresholds using the 10% variant-free and 90% variant-positive sample set (Data Supplement), models using Probe Set 3 appeared best for sensitivity. However, these models had unacceptably high false-positive rates with variant-free samples, whereas those for Probe Set 1 and 2 models were acceptable. This indicated that improved sensitivity for Probe Set 3 models could be due to looser thresholds from the thresholding process rather than additional probes providing subtle signals that the model used. When thresholds were determined using entirely variant-free samples, all models (Probe Set 1, 2, and 3) had the same target false-positive rate for variant-free samples, and sensitivities were more directly comparable. Hence, models using Probe Set 2 had optimal sensitivity (Fig 2) and were preferred over Set 3.

For RNA models, only Probe Sets 2 and 3 were tested. Probe Set 3 (used all RNA probes to call RNA variants) was the best-performing for RNA variants. Unlike DNA models, RNA

TABLE 2. Chosen Parameters for Top-Performing DNA and RNA Models

Variant Type	Training Set	Probe Set	C	Scale	Median LoD95	Observed Sensitivity	Observed FPR/Sample	Estimated FPR/Sample
Variants detected from DNA	3	2	0.01	0.6×	0.44% ± 0.16%	89% ± 6%	0.09% ± 0.09%	0.08% ± 0.07%
Gene fusions detected from RNA	4	3	0.01	0.6×	0.5 ± 0.6 copies	95.8% ± 0.8%	0.04% ± 0.04%	0.017% ± 0.018%
MET exon 14 skipping					69 ± 25 copies			

NOTE. Performance estimated using cross-validation.
Abbreviations: FPR, false-positive rate; LoD95, 95% limit of detection.

TABLE 3. Summary of Characteristics of the Final Model Selected for Use With Aspyre Lung Blood

Variant	LoD95 Estimated by Hit Rate	LoD95 Estimated by Linear Regression
SNVs/MNVs/indels (DNA)	0.2% VAF	0.19% ± 0.06% VAF
Gene fusions (RNA)	6 copies	1 amplifiable copy
MET exon 14 skipping (RNA)	160 copies	15 ± 24 copies

NOTE. Results are from verification experiments that used different reagent and sample batches and independent assay runs, distinct from those used during training.
Abbreviations: LoD95, 95% limit of detection; MNV, multinucleotide variation; SNV, single nucleotide variant; VAF, variant allele frequency.

models using Probe Set 3 had similar false-positive rates for variant-free and variant-positive samples, considering high uncertainty of the measurement. The greatest performance gains for RNA models were from varying the training data set. The removal of historical data improved RNA models such that median LoD95 for gene fusions was deemed one amplifiable copy; data removed included those generated with known probe-probe contamination.

TABLE 4. False-Positive Rate Assessment in Healthy Volunteer Samples

Category	No. Tested per ASPYRE Assay	No. Total Tested	No. False Positive
Samples	1	Total: 176 Standard input: 56 Low input: 120	0
Total nucleotide variants tested	114	20,064	0
SNVs	26	4,576	0
Indels + complex substitutions	31 + 20	8,976	0
Fusions	36	6,336	0
Exon skipping	1	176	0
Reportable variants	71	12,496	0

NOTE. A total of 176 nucleic acid samples from 50 variant free blood samples were tested for all variants covered by the Aspyre Lung panel. Standard Aspyre Lung input cfDNA: 20 ng and cfRNA: 42 ng; low Aspyre Lung input tested cfDNA: 5 ng and cfRNA: 6 ng. A single reportable variant may cover multiple nucleotide variants where the associated therapeutics are identical. For example, all gene fusions that involve *NTRK1*, *NTRK2*, or *NTRK3* will be reported under a single reportable variant as an *NTRK1/2/3* fusion biomarker. The total number of nucleotide variants tested is therefore higher than the number of reportable variants.
Abbreviations: cfDNA, cell-free DNA; cfRNA, cell-free RNA; SNV, single nucleotide variant.

After final model selection, we verified sensitivity using an independent sample batch and report a median LoD95 of 0.19% ± 0.06% for SNVs/MNVs/indels, one amplifiable copy for gene fusions, and 15 copies of *MET* exon 14 skipping events based on linear regression. *MET* exon 14 skipping copy numbers tested were 120, 160, 200, and 240, substantially higher than 15 copies, rendering this estimate unreliable. During model selection, an LoD95 of 69 copies was estimated using cross-validated data containing copy numbers above and below 69 (compare regression lines, Data Supplement), and consequently 69 copies are probably more realistic (Table 2). Gene fusion LoD95 estimates from hit rate and linear regression differ by six-fold; this difference is explicable as one amplifiable copy per sample 95% of the time requires approximately three copies on average (assuming Poisson distribution[21]); as cfRNA is fragmented,[22] six copies on average (i.e. two-fold higher) to achieve one amplifiable copy might be required.

Assay specificity was validated using a limit-of-blank study, demonstrating zero false positives across 20,000+ variant calls, even at low input; this specificity highlights the precision of pyrophosphorolysis.

While molecular assays have transformed precision oncology, all platforms have limitations. Aspyre Lung focuses on detection of guideline-recommended actionable variants for NSCLC and may not detect low-prevalence alterations, uncharacterized gene fusions, or variants associated with nonapproved therapeutics for potential off-label prescription (eg, *FGFR*, *NRAS*). Aspyre Lung requires PCR and real-time thermocyclers with no specialized equipment; however, physical separation of pre- and post-PCR steps is recommended, which is challenging in laboratories with limited space. Currently, the assay is validated for 384-well plates and manual pipetting although automation and 96-well plate formats are in development. Analysis optimization involved producing all samples in a range of VAFs or copy numbers for algorithm testing and training. Adding or removing variants therefore involves reproducing work described herein, which is nontrivial but not prohibitive.

In summary, Aspyre Lung provides a transformative, machine learning–powered solution for molecular testing in NSCLC. The combination of sensitivity, specificity, and accessibility uniquely addresses critical gaps in precision oncology, offering a practical and scalable alternative to more complex platforms. The streamlined single workflow for tissue and plasma enables adoption by a range of laboratories, including those with limited infrastructure, expanding access to high-quality molecular testing, and supporting clinicians in making timely, informed decisions. Analytical validation of Aspyre Clinical Test for Lung (Blood) laboratory developed test is complete[14]; further validation using clinical samples is ongoing, including through collaborations with external partners. Future work will focus on expanded clinical applications and exploring the assay's potential for improving patient outcomes.

AFFILIATIONS

[1]Biofidelity Ltd, Cambridge, United Kingdom
[2]Biofidelity Inc, Morrisville, NC

CORRESPONDING AUTHOR

Barnaby W. Balmforth, MPhys, PhD; e-mail: b.balmforth@biofidelity.com.

PRIOR PRESENTATION

Presented in part at the Association for Molecular Pathology Annual Meeting (AMP 2024), Vancouver, Canada, November 19-23, 2024.

SUPPORT

Supported by funding from Biofidelity Ltd.

DATA SHARING STATEMENT

A data sharing statement provided by the authors is available with this article at DOI https://doi.org/10.1200/CCI-25-00050.

AUTHOR CONTRIBUTIONS

Conception and design: Rebecca N. Palmer, Sam Abujudeh, Magdalena Stolarek-Januszkiewicz, Ana-Luisa Silva, Eleanor R. Gray, Robert J. Osborne, Barnaby W. Balmforth
Administrative support: Barnaby W. Balmforth
Collection and assembly of data: Rebecca N. Palmer, Magdalena Stolarek-Januszkiewicz, Ana-Luisa Silva, Justyna M. Mordaka, Kristine von Bargen, Alejandra Collazos, Simonetta Andreazza, Nicola D. Potts, Chau Ha Ho, Iyelola Turner, Jinsy Jose, Dilyara Nugent, Prarthna Barot, Christina Xyrafaki, Ryan T. Evans, Katherine E. Knudsen, Elizabeth Gillon-Zhang, Julia N. Brown, Candace King, Cory Kiser, Mary Beth Rossi, Eleanor R. Gray
Data analysis and interpretation: Rebecca N. Palmer, Sam Abujudeh, Magdalena Stolarek-Januszkiewicz, Alessandro Tomassini, Mary Beth Rossi, Eleanor R. Gray, Robert J. Osborne
Manuscript writing: All authors
Final approval of manuscript: All authors
Accountable for all aspects of the work: All authors

AUTHORS' DISCLOSURES OF POTENTIAL CONFLICTS OF INTEREST

The following represents disclosure information provided by authors of this manuscript. All relationships are considered compensated unless otherwise noted. Relationships are self-held unless noted. I = Immediate Family Member, Inst = My Institution. Relationships may not relate to the subject matter of this manuscript. For more information about ASCO's conflict of interest policy, please refer to www.asco.org/rwc or ascopubs.org/cci/author-center.
Open Payments is a public database containing information reported by companies about payments made to US-licensed physicians (Open Payments).

Rebecca N. Palmer
Employment: Biofidelity
Stock and Other Ownership Interests: Biofidelity, Lightcast Discovery Ltd
Research Funding: Biofidelity

Sam Abujudeh
Employment: Biofidelity, BenevolentAI
Stock and Other Ownership Interests: Biofidelity, BenevolentAI
Research Funding: Biofidelity, BenevolentAI

Magdalena Stolarek-Januszkiewicz
Employment: Biofidelity
Stock and Other Ownership Interests: Biofidelity
Honoraria: Biofidelity
Research Funding: Biofidelity
Patents, Royalties, Other Intellectual Property: I am a co-author of one or more patents related to published technology. These patents are relevant to the subject matter of this work and may be associated with potential financial interests. I have no direct financial interest in the royalties or commercialization of these patents at this time, but I disclose this involvement for transparency
Expert Testimony: Biofidelity
Travel, Accommodations, Expenses: Biofidelity

Ana-Luisa Silva
Employment: Biofidelity
Stock and Other Ownership Interests: Biofidelity
Research Funding: Biofidelity

Justyna M. Mordaka
Employment: Biofidelity
Stock and Other Ownership Interests: Biofidelity
Research Funding: Biofidelity
Travel, Accommodations, Expenses: Biofidelity

Kristine von Bargen
Employment: Biofidelity
Stock and Other Ownership Interests: Biofidelity
Research Funding: Biofidelity

Alejandra Collazos
Employment: Biofidelity, Tessellate Bio Ltd (I)
Stock and Other Ownership Interests: Biofidelity, Tessellate Bio Ltd (I)
Research Funding: Biofidelity
Patents, Royalties, Other Intellectual Property: Royalty regarding patent on DNS PK inhibitor with Newcastle University and AstraZeneca (I)

Simonetta Andreazza
Employment: Biofidelity, AstraZeneca (I)
Stock and Other Ownership Interests: Biofidelity, AstraZeneca (I)
Research Funding: Biofidelity

Nicola D. Potts
Employment: Biofidelity
Stock and Other Ownership Interests: Biofidelity

Chau Ha Ho
Employment: Biofidelity
Stock and Other Ownership Interests: Biofidelity
Research Funding: Biofidelity

Iyelola Turner
Employment: Biofidelity
Stock and Other Ownership Interests: Biofidelity
Research Funding: Biofidelity
Travel, Accommodations, Expenses: Biofidelity

Jinsy Jose
Employment: Biofidelity
Stock and Other Ownership Interests: Biofidelity
Research Funding: Biofidelity

Dilyara Nugent
Employment: Biofidelity
Stock and Other Ownership Interests: Biofidelity
Research Funding: Biofidelity (Inst)

Prarthna Barot
Employment: Biofidelity
Stock and Other Ownership Interests: Biofidelity
Research Funding: Biofidelity

Christina Xyrafaki
Employment: Biofidelity
Stock and Other Ownership Interests: Biofidelity
Research Funding: Biofidelity
Travel, Accommodations, Expenses: Biofidelity

Alessandro Tomassini
Employment: Biofidelity
Stock and Other Ownership Interests: Biofidelity
Research Funding: Biofidelity

Ryan T. Evans
Employment: Biofidelity
Stock and Other Ownership Interests: Biofidelity
Research Funding: Biofidelity
Travel, Accommodations, Expenses: Biofidelity

Katherine E. Knudsen
Employment: Biofidelity
Stock and Other Ownership Interests: Biofidelity
Research Funding: Biofidelity
Travel, Accommodations, Expenses: Biofidelity

Elizabeth Gillon-Zhang
Employment: Biofidelity
Stock and Other Ownership Interests: Biofidelity
Research Funding: Biofidelity (Inst)

Julia N. Brown
Employment: Biofidelity
Stock and Other Ownership Interests: Biofidelity
Research Funding: Biofidelity

Candace King
Stock and Other Ownership Interests: Biofidelity

Cory Kiser
Employment: Biofidelity Inc, IQvia, Q2 Solutions—Genomics Lab, Genomic Services
Research Funding: Biofidelity

Mary Beth Rossi
Employment: Biofidelity

Eleanor R. Gray
Employment: Biofidelity
Stock and Other Ownership Interests: Biofidelity
Research Funding: Biofidelity

Robert J. Osborne
Employment: Biofidelity, Biomodal Ltd
Leadership: Biofidelity, Biomodal Ltd
Stock and Other Ownership Interests: Biofidelity, Biomodal Ltd

Barnaby W. Balmforth
Employment: Biofidelity
Leadership: Biofidelity
Stock and Other Ownership Interests: Biofidelity
Travel, Accommodations, Expenses: Biofidelity

No other potential conflicts of interest were reported.

REFERENCES

1. National Comprehensive Cancer Network: NCCN Clinical Practice Guidelines in Oncology (NCCN Guidelines): Non-Small Cell Lung Cancer, Version 3. 2025. www.nccn.org
2. Scott JA, Lennerz J, Johnson ML, et al: Compromised outcomes in stage IV non–small-cell lung cancer with actionable mutations initially treated without tyrosine kinase inhibitors: A retrospective analysis of real-world data. JCO Oncol Pract 20:145-153, 2024
3. Chen Y, Carlson A: Abstract 3426: Real-world biomarker testing rates and trends among patients with advanced non-small cell lung cancer in the US. Cancer Res 84:3426, 2024
4. Rolfo C, Mack P, Scagliotti GV, et al: Liquid biopsy for advanced NSCLC: A consensus statement from the International Association for the Study of Lung Cancer. J Thorac Oncol 16:1647-1662, 2021
5. Sadik H, Pritchard D, Keeling D-M, et al: Impact of clinical practice gaps on the implementation of personalized medicine in advanced non–small-cell lung cancer. JCO Precis Oncol 6:e2200246, 2022
6. Wan JCM, Massie C, Garcia-Corbacho J, et al: Liquid biopsies come of age: Towards implementation of circulating tumour DNA. Nat Rev Cancer 17:223-238, 2017
7. Byfield SD, Bapat B, Becker L, et al: Real-world analysis of commercially insured and Medicare Advantage patients with advanced cancer and rates of molecular testing. J Clin Oncol 41:6633, 2023
8. Evangelist MC, Butrynski JE, Paschold JC, et al: Contemporary biomarker testing rates in both early and advanced NSCLC: Results from the MYLUNG pragmatic study. J Clin Oncol 41:9109, 2023
9. Hagemann IS, Devarakonda S, Lockwood CM, et al: Clinical next-generation sequencing in patients with non–small cell lung cancer. Cancer 121:631-639, 2015
10. Megahed AI, Zheng D, Chen LH, et al: Half of oncologists fail to use ordered NGS results to guide their first-line treatment decision in advanced NSCLC: A retrospective study in a community-based integrated healthcare system. Heliyon 10:e36308, 2024
11. Penault-Llorca F, Socinski MA: Emerging molecular testing paradigms in non-small cell lung cancer management—Current perspectives and recommendations. Oncologist 30:oyae357, 2025
12. Evans RT, Gillon-Zhang E, Brown JN, et al: ASPYRE-Lung: Validation of a simple, fast, robust and novel method for multi-variant genomic analysis of actionable NSCLC variants in FFPE tissue. Front Oncol 14:1420162, 2024
13. Gray ER, Mordaka JM, Christoforou ER, et al: Ultra-sensitive molecular detection of gene fusions from RNA using ASPYRE. BMC Med Genomics 15:215, 2022
14. Evans RT, Knudsen KE, Gillon-Zhang E, et al: Analytical validation of Aspyre Clinical Test for Lung (Blood): A multiplexed PCR and pyrophosphorolysis-based assay for detecting actionable NSCLC variants in plasma cfDNA and cfRNA. J Liq Biopsy 8:100298, 2025
15. Pabinger S, Rödiger S, Kriegner A, et al: A survey of tools for the analysis of quantitative PCR (qPCR) data. Biomol Detect Quantif 1:23-33, 2014
16. Yuan JS, Reed A, Chen F, et al: Statistical analysis of real-time PCR data. BMC Bioinformatics 7:85, 2006
17. Silva A-L, Powalowska PK, Stolarek M, et al: Single-copy detection of somatic variants from solid and liquid biopsy. Sci Rep 11:6068, 2021
18. Abbosh C, Birkbak NJ, Swanton C: Early stage NSCLC—Challenges to implementing ctDNA-based screening and MRD detection. Nat Rev Clin Oncol 15:577-586, 2018
19. Diehl F, Schmidt K, Choti MA, et al: Circulating mutant DNA to assess tumor dynamics. Nat Med 14:985-990, 2008
20. Bredno J, Lipson J, Venn O, et al: Clinical correlates of circulating cell-free DNA tumor fraction. PLoS One 16:e0256436, 2021
21. He Y, Xie T, Tu Q, et al: Importance of sample input volume for accurate SARS-CoV-2 qPCR testing. Anal Chim Acta 1199:339585, 2022
22. Johnston AD, Lu J, Korbie D, et al: Modelling clinical DNA fragmentation in the development of universal PCR-based assays for bisulfite-converted, formalin-fixed and cell-free DNA sample analysis. Sci Rep 12:16051, 2022